

Generating Data Locality to Accelerate Sparse Matrix-Matrix Multiplication on CPUs

Jordi Wolfson-Pou

Intel

Santa Clara, CA, USA

jordi.wolfson-pou@intel.com

Jan Laukemann

Erlangen National High Performance Computing Center

University of Erlangen-Nürnberg

Erlangen, Germany

jan.laukemann@fau.de

Fabrizio Petrini

Intel

Santa Clara, CA, USA

fabrizio.petrini@intel.com

Abstract—Sparse General Matrix-matrix Multiplication (SpGEMM) is a critical operation in many applications. Current multithreaded implementations are based on Gustavson’s algorithm and often perform poorly on large matrices due to limited cache reuse by the accumulators. We present MAGNUS (Matrix Algebra for Gigantic Numerical Systems), a novel algorithm to maximize data locality in SpGEMM. To generate locality, MAGNUS reorders the intermediate product into discrete cache-friendly chunks using a two-level hierarchical approach. The accumulator is applied to each chunk, where the chunk size is chosen such that the accumulator is cache-efficient. MAGNUS is input- and system-aware: based on the matrix characteristics and target system specifications, the optimal number of chunks is computed by minimizing the storage cost of the necessary data structures. MAGNUS allows for a hybrid accumulation strategy in which each chunk uses a different accumulator based on an input threshold. We consider two accumulators: an AVX-512 vectorized bitonic sorting algorithm and classical dense accumulation. An OpenMP implementation of MAGNUS is compared with several baselines for a variety of different matrices on three Intel x86 architectures. For matrices from the SuiteSparse collection, MAGNUS is faster than all the baselines in most cases and is orders of magnitude faster than Intel MKL for several matrices. For massive random matrices that model social network graphs, MAGNUS scales to the largest matrix sizes, while the baselines fail to do so. Furthermore, MAGNUS is close to the optimal bound for these matrices, regardless of the matrix size, structure, and density.

Index Terms—Sparse matrix, SpGEMM, x86, non-temporal streaming, vector processor, AVX-512

I. INTRODUCTION

The sparse general matrix-matrix multiplication operation (SpGEMM) $C = AB$ is critical to the performance of many applications, including genome assembly [24], [25], [44], machine learning [6], [18], [39], [40], algebraic multigrid [17], [30], and graph analytics [5], [21], [22], [27], [29], [43]. The challenge of SpGEMM comes from the sparsity structures of A and B , which create unpredictable access patterns. This is problematic for modern multi-core architectures, which are designed for regular accesses and high data reuse. As a result, many state-of-the-art SpGEMM algorithms scale poorly to massive irregular matrices due to ineffective use of the cache hierarchy.

Multithreaded SpGEMM algorithms are typically based on Gustavson’s method, where rows of B are loaded, scaled, and

accumulated (equivalently, summed or merged) for each row of A . From load balancing to vectorized algorithms, optimizing the accumulation step has been the primary focus of research on Gustavson’s method. There are two types of accumulators: dense and sparse. Dense accumulators involve a data structure of the size of the number of columns of C and perform well in cases where the entire dense array is loaded infrequently (for example, banded matrices). Sparse accumulators use more compact containers, for example, hash map or sort-based strategies. However, hash map-based accumulators experience caching issues due to probing and dynamic re-sizing, and the performance of sort-based methods significantly drops as the number of elements increases, which is problematic when many elements must be merged.

Several algorithms were derived to improve caching issues in accumulators, the most recent being the CSeg method [2], [38]. The core idea is to partition the columns of B so that the range of column indices in each partition allows the accumulator to fit in cache, where data structures that store partitioning information are constructed during a setup phase. However, these methods can scale poorly for some datasets; if there are many partitions, the performance of the construction and access to the extra data structures can be high, especially since the number of partitions grows with the matrix dimensions.

We present MAGNUS (Matrix Algebra for Gigantic Numerical Systems), a novel algorithm that uses a hierarchical approach to generate the locality needed by the accumulators. To achieve this, the intermediate product of C is reordered into cache-friendly chunks that are processed independently by the accumulator. The MAGNUS workflow consists of two main algorithms: the fine- and coarse-level algorithms. The coarse-level algorithm is based on the outer product formulation of SpGEMM and generates the first layer of locality by reordering the *intermediate product* (arrays of column indices and values generated before accumulation) into smaller chunks. The fine-level algorithm is based on Gustavson’s formulation and further reorders the coarse-level chunks. The accumulator is then applied to each fine-level chunk. MAGNUS is input- and system-aware: the number of fine- and coarse-level chunks are chosen based on the matrix and system cache sizes, where the optimal number of chunks is chosen by minimizing the storage cost of the data structures in MAGNUS. In the accumulation

stage, we use a hybrid approach, where AVX-512 vectorized sorting is used on chunks with a small number of elements, and dense accumulators are used on large chunks.

An OpenMP implementation of MAGNUS is compared with several baselines, including the Intel Math Kernel Library (MKL) [10], CSeg [2], and Hash and Heap based accumulators [34], [35]. Three matrix test sets are evaluated on three Intel x86 architectures. For the SuiteSparse matrix collection [13], MAGNUS is the fastest method in most cases and is orders of magnitude faster than MKL in some cases. For our second matrix set, which comes from a recursive model to generate power law graphs [8], we show that MKL does not scale with matrix size, while MAGNUS and CSeg do, with MAGNUS having the fastest overall time. Lastly, we consider massive uniform random matrices (i.e., matrices from the Erdős–Rényi (ER) model [16]), which is the most challenging case for our baselines, since the uniformity results in the loading of the entire accumulation array. This test set demonstrates the need for the two-level approach in MAGNUS, where using the fine-level algorithm alone results in divergence from an ideal performance bound (CSeg also exhibits this poor scaling). However, using the full MAGNUS algorithm allows scaling to the largest case, where the performance of MAGNUS is close to an ideal bound independent of the matrix size.

II. BACKGROUND

A. Preliminaries and Definitions

Let C be a sparse matrix with $n(C)$ rows, $m(C)$ columns, and $nnz(C)$ number of non-zero values. The general sparse matrix-matrix multiplication (SpGEMM) operation is defined as

$$C = \alpha A \cdot B + \beta C, \quad (1)$$

where α and β are scalars. The operation $A \cdot B$ is the dominant cost and is itself often referred to as SpGEMM.

B. Gustavson’s Method

Multi-threaded implementations of SpGEMM are typically based on Gustavson’s row-by-row algorithm [26]. Let $\mathcal{S}(A_i)$ be the set of column indices corresponding to the non-zero values in row i of A . Row i for $0 \leq i \leq n(C)$ of C is computed as:

$$C_i = \sum_{j \in \mathcal{S}(A_i)} A_{ij} B_j, \quad (2)$$

i.e., for some row i of C , the rows of B are scaled by the non-zeros in row i of A . These scaled rows are then summed together to give the final row of C . Since each row of C is computed independently, multithreaded implementations typically partition rows among threads, which is the approach we take for MAGNUS.

There are two main ingredients for implementing Gustavson’s method: the matrix storage scheme and the algorithm that *accumulates* the scaled rows of B . Compressed sparse row (CSR) format is one of the most popular storage schemes and is especially useful for algorithms such as Gustavson’s method that traverse matrices row-by-row. CSR requires three arrays:

$C.col$, $C.val$, and $C.rowPtr$. The arrays $C.col$ and $C.val$ of size $nnz(C)$ store the column indices and values (with data types `idx_t` and `val_t`), respectively, of the non-zero values of C . The array $C.rowPtr$ of size $n(C) + 1$ stores the starting positions in $C.col$ and $C.val$ of the rows.

Algorithm 1 shows pseudo code for the *numeric phase* of the CSR-based Gustavson method with a *dense accumulator*, where the variables in bold are global. The column indices in the row i of A are loaded as $idx = A.col[A.rowPtr[i]]$, and the rows of B are loaded by reading $B.col$ from $B.rowPtr[idx]$ to $B.rowPtr[idx + 1]$. A dense array $accumBuff$ of size $m(C)$ is updated for each column index of B , a companion bitmap stores the non-zero positions in $accumBuff$, and $colBuff$ stores the running list of column indices in C . Besides A , B and C , all data structures are thread-local. In some modern SpGEMM algorithms, such as expand-sort-compress (ESC) [12], [23], two phases are performed, where the *intermediate product* of C is written to an array instead of directly updating the accumulator. The intermediate product is generated in the first loop by storing $B.col[k]$ and $A.val[j] * B.val[k]$ in temporary buffers. This allows for more types of accumulation strategies, such as sort-based algorithms.

Algorithm 1: Gustavson’s with Dense Accumulation

```

1 for  $i \leftarrow 0$  to  $n - 1$  do in parallel
2    $count \leftarrow 0$ 
3   /* read row  $i$  of  $A$  */
4   for  $j \leftarrow A.rowPtr[i]$  to  $A.rowPtr[i + 1] - 1$  do
5     /* read row  $j$  of  $B$  */
6     for  $k \leftarrow B.rowPtr[A.col[j]]$  to
7        $B.rowPtr[A.col[j] + 1] - 1$  do
8       /* multiply and update accumulator */
9        $accumBuff[B.col[k]] +=$ 
10         $A.val[j] * B.val[k]$ 
11       if  $bitMap[B.col[k]] == 0$  then
12          $colBuff[count++] = B.col[k]$ 
13          $bitMap[B.col[k]] \leftarrow 1$ 
14       end
15     end
16   end
17   /* write to  $C$  */
18    $k \leftarrow C.rowPtr[i]$ 
19   for  $j \in colBuff$  do
20      $C.col[k] \leftarrow j$ 
21      $C.val[k++] \leftarrow accumBuff[j]$ 
22      $bitMap[j] \leftarrow 0$ 
23   end
24 end

```

SpGEMM requires a *symbolic* phase before the numeric phase to compute $C.rowPtr$. Typically, the symbolic phase follows the same algorithm as the numeric phase but without updating $accumBuff$, $colBuff$, $C.col$, and $C.val$. Instead, only the bitmap is updated along with a counter that outputs the exact number of non-zeros for each row of C . Finally, a prefix sum on the counters computes $C.rowPtr$. This type of symbolic phase is known as *precise prediction*, where the number of non-zeros of C is computed exactly before the numeric phase. Although there are other approaches to

computing the C metrics [1], [12], [20], [32], [33], precise prediction is adopted by popular libraries such as MKL [10] and cuSPARSE [11] due to its minimal memory requirements.

C. Related Work

Optimizations related to the accumulation step have been the primary focus of research on SpGEMM. For load balancing, a common approach is based on the observation that rows with different intermediate sizes require different accumulation strategies [9], [12], [15], [23], [32], [33], [36], [37]. In [12], A is reordered by increasing intermediate size. Other approaches group rows based on the size of the intermediate product, where a different accumulator is used for different groups [9], [15], [32], [33], [36], [37], [42]. In [32], five different accumulation strategies are used, including priority queues and sorting algorithms.

Developing new accumulators is another topic that has been widely studied, especially for modern multicore machines with vector processors [7], [28], [34], [35], [41], [45], [46]. A common approach is to optimize sorting algorithms [7], [12], [23], [29], [31], [33] or data structures such as heaps [4], [34], [35] and hash maps [3], [11], [14], [31], [34], [35], [40]. In MAGNUS, a combination of vectorized sorting [7] and classical dense accumulation [20] is used. In Section IV-C, MAGNUS is compared with hash map and heap-based approaches, which are considered state-of-the-art [2], [10], [34], [35].

Perhaps most relevant to MAGNUS are recent works on improving the cache behaviour of accumulators, proposed in [38] and improved in the CSeg method [2]. The core concept is to partition the columns of B into segments, where the number of segments is chosen such that the dense accumulator fits into cache. CSeg was shown to be overall faster than many state-of-the-art libraries mentioned earlier. For a more extensive overview of SpGEMM research, including distributed memory algorithms, see [19].

III. MAGNUS

A. Overview

MAGNUS uses a novel hierarchical algorithm, where two levels of locality are generated. The *coarse-level algorithm* reorders the intermediate product into discrete chunks and the *fine-level algorithm* further reorders and accumulates the coarse-level chunks. The reordering is based on optimal parameters that are computed using the input matrix properties and the target system specifications. These parameters are optimal in the sense that they minimize the storage cost of all necessary data structures. The levels are generated using a set of basic operations, including histogramming and prefix summing. The combination of the building blocks with MAGNUS’s optimal parameters results in cache-efficient accumulators.

The coarse- and fine-level algorithms are combined when multiplying “massive” matrices, i.e., matrices in which the data structures required by the fine-level algorithm does not fit into cache (this will be discussed in Section III-E). For smaller matrices, the fine-level algorithm is used alone, which avoids the $2\times$ additional data volume incurred by first applying the

coarse-level algorithm. When used together, the coarse-level is generated using an outer product-based algorithm, which is the source of the additional data volume. When the fine-level algorithm is used alone, we use a modified Gustavson’s algorithm. Since the intermediate product is generated in both cases, MAGNUS can be thought of as an ESC-type algorithm [12].

Our strategies for generating locality also simplify load balancing. Since our accumulation is performed on cached data, the dominant cost is simply reading A and B and writing to C . Therefore, we simply partition the rows among threads (as in standard Gustavson-based algorithms) such that the total number of intermediate elements per thread is balanced. Our approach uses precise prediction for the symbolic phase, but for brevity we will only describe the numeric phase. See section II for clarity on the differences between the symbolic and numeric phases.

Figure 1 shows a simple workflow for MAGNUS, where two threads are used to multiply two 8×8 matrices. The example shows how row one and two assigned to thread t_0 are computed, where two chunks are used for both the coarse and fine levels. The outer product-based approach traverses the submatrix of A (corresponding to rows one and two) column by column, and the highlighted rows of B are traversed row by row. This traversal generates the four coarse-level chunks, which are processed one-by-one. Each chunk is reordered again to get the eight fine-level chunks, where the accumulator is applied to get the final result for rows one and two. Note that all coarse-level chunks are generated before performing the fine-level algorithm. However, the fine level is processed depth-first; for each coarse-level chunk, the fine level is generated and then immediately accumulated before moving to the next coarse-level chunk.

In the example, the coarse-level algorithm is applied only to rows one and two, which is by design. In a pre-processing step, MAGNUS categorizes each row based on the structure of the row and the system specifications:

- 1) **Sort:** if the number of intermediate elements is less than the dense accumulation threshold, we can directly apply a sort-based accumulator without reordering. The dense accumulation threshold will be described later in this section.
- 2) **Dense accumulation:** if the *intermediate row length* fits into the L2 cache, we can directly apply dense accumulation to the row without reordering since the range of column indices of row i of C does not exceed the size of the L2 cache. The intermediate row length is defined as the difference between the minimum and maximum column index in the intermediate product.
- 3) **Fine level:** if $s_{finelevel} < s_{L2}$, the fine-level algorithm can be applied, where $s_{finelevel}$ is the number of bytes required to store all necessary fine-level data structures.
- 4) **Coarse level:** the coarse-level algorithm is applied to all remaining rows, where the fine-level algorithm is applied to each coarse-level chunk.

The accumulation parameters mentioned above will be discussed in Section III-D, including a description of the sorting algorithm. The first two categories imply that some rows possess intrinsic locality and do not require the algorithms in MAGNUS. Once each row is categorized, each thread traverses its rows category-first to ensure that data specific to a particular category is cached for as long as possible.

For simplicity, we assume $m(C)$ is a power of two in our descriptions of the algorithms in MAGNUS. In our implementation of MAGNUS, $m(C)$ is ceiled to the nearest power of two to allow efficient bitwise operations.

B. The Fine-level Algorithm

The fine-level algorithm has the following steps for each row: histogram, prefix sum, reorder, and accumulate. As in Gustavson’s method, each row (or coarse-level chunk in cases where the coarse-level algorithm is applied) is computed before moving on to the next row. This means that the intermediate product is only generated for a single row (or coarse-level chunk at any given time), unlike in outer product-based approaches.

The pseudocode is shown in Algorithm 2, and an example is shown in Figure 2. In the example, the input is two arrays of column indices and values, which are generated by the coarse-level algorithm. However, for rows that only require fine-level locality, A and B are read directly as in Algorithm 1, i.e., the loop headers on lines 3 and 11 of Algorithm 2 are replaced with the nested headers on lines 4 and 6 of Algorithm 1.

Algorithm 2: MAGNUS fine-level algorithm applied to a single coarse-level chunk

```

Input:  $colCoarse, valCoarse$ 
Output:  $C_{i, rangeCoarse}$ 
1 /* histogram */
2  $countsFine \leftarrow 0$ 
3 for  $col \in colCoarse$  do
4    $chunk \leftarrow col \ll chunkShiftFine$ 
5    $countsFine[chunk]++$ 
6 end
7 /* prefix sum */
8  $offsetsFine[0] = 0$ 
9  $\&offsetsFine[1] \leftarrow inclusiveScan(countsFine)$ 
10 /* reorder */
11  $counts \leftarrow 0$ 
12 for  $\{col, val\} \in \{colCoarse, valCoarse\}$  do
13    $chunk \leftarrow col \ll chunkShiftFine$ 
14    $\ell \leftarrow offsetsFine[chunk] + countsFine[chunk]++$ 
15    $colFine[\ell] \leftarrow col - chunk * chunkLenFine$ 
16    $valFine[\ell] \leftarrow val$ 
17 end
18 /* accumulation */
19 for  $j \leftarrow 0$  to  $nChunksFine - 1$  do
20    $k \leftarrow offsetsFine[j]$ 
21    $C_{i, rangeFine_j} \leftarrow accum(\&colFine[k], \&valFine[k])$ 
22 end

```

The first step towards reordering the intermediate product is to compute the array $offsetsFine$, which stores the start and end locations of each fine-level chunk in the arrays $colFine$ and $valFine$. The histogram step is shown in lines

3-9 of Algorithm 2. The column indices are mapped to chunks as $col/chunkLenFine$, where $chunkLenFine = m(C)/nChunksFine$ denotes the local range of the column indices within a chunk. After the histogram is computed, a prefix sum (inclusive scan) of the histogram is performed to generate the chunk offsets.

To reorder the input (lines 14-22), the histogramming phase is repeated, where the histogram is used to track the current number of elements written to each chunk. Elements are reordered by writing the input coarse-level chunk at the position $offsetsFine[chunk] + countsFine[chunk]$ in $colFine$ and $valFine$. The column indices are shifted into the local range of each chunk as $col - chunk * chunkLenFine$ to allow for cache-efficient accumulation. After the accumulation step, the column indices are shifted back into the correct range before writing them to C . The variable $rangeFine_j$ denotes the range of column indices of the fine-level chunk j (i.e., $[j * chunkLenFine, (j + 1) * chunkLenFine)$), and $rangeCoarse$ is the range of column indices of the input coarse-level chunk.

Algorithm 2 shows that $countsFine$, $offsetsFine$, $colFine$ and $valFine$ are the only data structures needed in addition to A , B and C . Arrays $countsFine$ and $offsetsFine$ are of size $nChunksFine$, but $colFine$ and $valFine$ are of size $\max_{0 \leq i < n(C)} (\sum_{j \in S(A_i)} nnz(B_j))$, i.e., the row that produces the maximum number of intermediate elements. The extra memory required for $colFine$ and $valFine$, which typically dominates that of $countsFine$ and $offsetsFine$, is typical of ESC-type SpGEMM algorithms. Figure 2 shows the workflow of the fine-level algorithm in terms of the data structures from Algorithm 2. The input in this example is the first chunk from the example in Figure 1.

C. The Coarse-level Algorithm

As the columns of C increase, combined storage of the fine-level data structures eventually exceeds the size of the L2 cache. For such matrices, an initial coarse level must be generated, which provides the first layer of locality. To generate the coarse level, we use a modified outer product-based algorithm where the intermediate product is generated and reordered for all rows that require coarse-level locality before any accumulation occurs. The reordered intermediate product is organized into discrete chunks that can be handled independently by the fine-level algorithm.

Conventional outer product algorithms typically involve the generation of the intermediate product by multiplying columns of A stored in CSC format with rows of B stored in CSR format. For the coarse-level algorithm in MAGNUS, the outer product of a subset of rows is needed (those rows categorized as coarse-level rows). Therefore, a CSC version of the submatrix \hat{A} of A is constructed, where \hat{A} only includes the rows of A in the coarse-level category (i.e., those that require coarse-level locality). Each thread performs the following steps on its list of coarse-level rows stored in the array $coarseRowsC$:

- 1) For all $i \in coarseRowsC$, generate $coarseRowsB$, i.e., the unique set of rows in B required to perform the outer

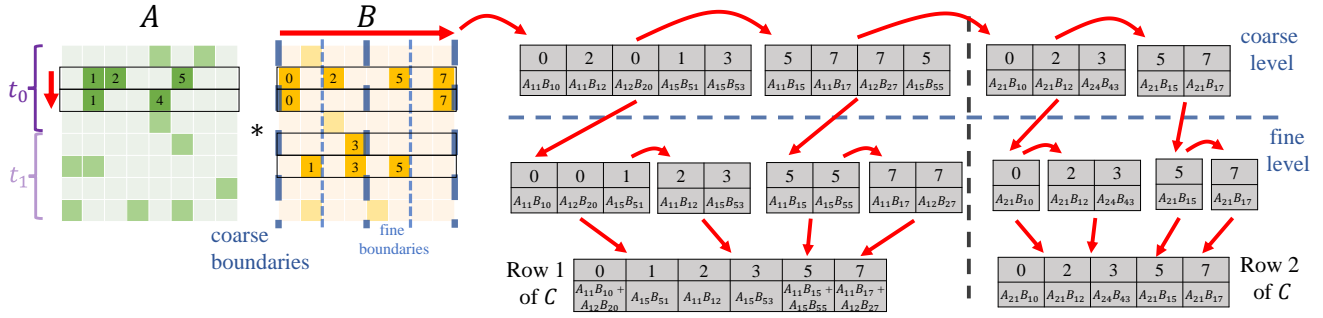


Fig. 1. Example workflow of MAGNUS, where two threads multiply two 8×8 matrices, where two coarse- and fine-level chunks are used. The example shows how rows one and two (assigned to thread t_0) are computed.

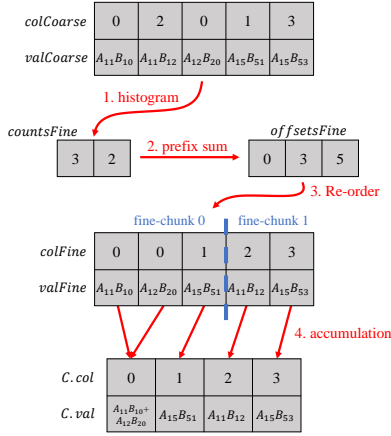


Fig. 2. Data structure-view of applying the fine-level algorithm to the first chunk from Figure 1.

product. This is done by iterating through the non-zeros of \hat{A} and setting a bitmap, where $coarseRowsB$ is the list of set bits.

- 2) Construct the CSC submatrix \hat{A}^{CSC} using the well-known approach for the conversion of CSR to CSC in which a histogramming stage computes the number of non-zeros per row, a prefix sum computes $colPtr$, and $colPtr$ is then used to construct the arrays row and val . This step is inexpensive since the complexity of outer product-based SpGEMM is dominated by the generation of the intermediate product in the next step. Specifically, the complexity of constructing \hat{A} is $O(nnz(A))$, while the complexity of generating the intermediate product is $O(nnz(A))$ in the best case and $O(nnz(A) * m(B))$ in the worst case.
- 3) Perform a histogram step by reading \hat{A}^{CSC} and the rows of B corresponding to $coarseRowsB$. Then a prefix sum on the histogram generates the coarse-level offsets.
- 4) Generate the coarse level by reading again \hat{A}^{CSC} , reading the rows of B corresponding to $coarseRowsB$, and writing the result in $colCoarse$ and $valCoarse$ at positions determined by the offsets.
- 5) For each coarse-level chunk, apply the fine-level algorithm.

Steps 3-5 are shown in Algorithm 3. The same set of

basic building blocks is used as in the fine-level algorithm (histogramming, prefix summing, and reordering). The key difference is that the chunks for all rows are generated at the same time. The prefix sum is modified to compute the chunk offsets within a row based on the offsets from the previous rows. In our implementations, we also use non-temporal stores to generate the coarse-level chunks to avoid polluting the cache. This allows us to retain the accumulator and fine-level data structures in cache while generating all the coarse-level chunks. In the final loop, the fine-level algorithm is applied to each coarse-level chunk for each row. Figure 3 shows the data structures for the example in Figure 1.

Similarly to other approaches based on the outer product, the memory requirement for the coarse-level algorithm is higher than the fine-level algorithm, since the intermediate product for multiple rows must be stored. In the worst case, the memory requirement is proportional to the sum of the outer products of all rows, which may exceed the memory capacity of certain memory-constrained systems. Therefore, we use a batching approach, where we collect rows of C into $coarseRowsC$ until one of two conditions is met: (1) the memory limit of our system is reached, or (2) the storage requirement for generating the coarse-level chunks ($countsCoarse$, $offsetsCoarse$, and small buffers for the non-temporal streaming stores) exceeds the L2 cache size. If either condition is met, the batch of rows in $coarseRowsC$ is computed via steps 2-5. This batching process is then repeated until all rows in the coarse-level algorithm category have been computed.

D. Accumulation

MAGNUS is accumulator-agnostic; only the storage requirement of the desired accumulators is needed to compute the optimal MAGNUS parameters. This allows portability and flexibility. For portability, accumulators optimized for specific architectures can be chosen without changing the locality-generation algorithms. This is evident in Algorithm 2, where the $accum()$ function only requires an input chunk. For flexibility, MAGNUS allows for a hybrid approach where each chunk chooses an accumulator based on the chunk characteristics. In this paper, we consider two accumulators: AVX-512 vectorized bitonic sorting [7] and classical dense accumulation. For chunks with a small number of elements,

Algorithm 3: MAGNUS coarse-level algorithm

Input: \hat{A}^{CSC} , B , $coarseRowsB$, $coarseRowsC$
Output: $C_{i,rangeCoarse_j}$

```

1 /* Histogram */
2 for  $i \in coarseRowsB$  do
3   for  $j \leftarrow \hat{A}^{CSC}.colPtr[i]$  to  $\hat{A}^{CSC}.colPtr[i+1] - 1$  do
4     for  $k \leftarrow B.rowPtr[i]$  to  $B.rowPtr[i+1] - 1$  do
5        $chunk \leftarrow B.col[k] \ll shiftCoarse$ 
6        $countsCoarse[\hat{A}^{CSC}.row[j]][chunk]++$ 
7     end
8   end
9 end
10 /* Prefix sum */
11  $offsetsCoarse[0][0] \leftarrow 0$ 
12 for  $i \in coarseRowsC$  do
13    $\&offsetsCoarse[i][1] \leftarrow$ 
14      $inclusiveScan(countsCoarse[i])$ 
15    $offsetsCoarse[i+1][0] \leftarrow$ 
16      $offsetsCoarse[i][nChunksCoarse]$ 
17 end
18 /* reordering */
19 for  $i \in coarseRowsB$  do
20   for  $j \leftarrow \hat{A}^{CSC}.colPtr[i]$  to  $\hat{A}^{CSC}.colPtr[i+1] - 1$  do
21     for  $k \leftarrow B.rowPtr[i]$  to  $B.rowPtr[i+1] - 1$  do
22        $chunk \leftarrow B.col[k] \ll shiftCoarse$ 
23        $\ell \leftarrow offsetsCoarse[\hat{A}^{CSC}.row[j]][chunk] +$ 
24          $countsCoarse[\hat{A}^{CSC}.row[j]][chunk]++$ 
25       /* Write chunks using non-temporal stores */
26        $colChunks[\ell] \leftarrow$ 
27          $B.col[k] - chunk * chunkLenCoarse$ 
28        $valChunks[\ell] \leftarrow \hat{A}^{CSC}.val[j] * B.val[k]$ 
29     end
30   end
31 end
32 /* Apply fine-level algorithm to each coarse-level chunk */
33 for  $i \in coarseRowsC$  do
34   for  $j \leftarrow 0$  to  $nChunksCoarse - 1$  do
35      $k \leftarrow offsetsCoarse[i][j]$ 
36      $C_{i,rangeCoarse_j} \leftarrow$ 
37        $fineLevel(\&colCoarse[k], \&valCoarse[k])$ 
38   end
39 end

```

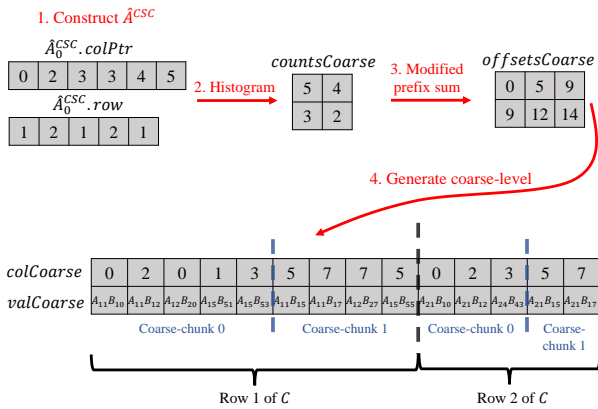


Fig. 3. Data structure-view of the coarse-level algorithm for the example from Figure 1.

sorting is performed; otherwise, classical dense accumulation is used. When visiting each chunk, a threshold is used to choose the accumulator. This threshold is based on how the sorting algorithm is implemented: quicksort is used to partition the array, and then hard-coded vectorized bitonic sorting networks are used to sort the partitions. We found experimentally that dense accumulation is faster than sorting unless the sort size is small enough to bypass quicksort and directly use bitonic sort. For more details, see Section IV-B1 and [7].

E. Choosing the Number of Chunks

The optimal number of chunks is chosen based on the system specifications and the input matrix properties, where the cache line and L2 sizes, $s_{cacheLine}$ and s_{L2} , respectively, are input parameters based on the target system. For simplicity, assume $m(C)$ is a power of two ($m(C)$ is ceiled to the nearest power of two otherwise). Choosing the optimal number of fine-level chunks corresponds to minimizing the function

$$\frac{m(C) * s_{denseAccum}}{nChunksFine} + nChunksFine * (s_{chunkFine}), \quad (3)$$

i.e., minimizing the storage required by the fine-level algorithm, where $nChunksFine$ is a free parameter. The first term is the storage requirement of the dense accumulator, where the number of elements in the dense accumulator array is $m(C)/nChunksFine$. For the numeric phase, $s_{denseAccum} = s_{val} + 1$ since values are accumulated and a bit map is updated. For the symbolic phase, $s_{denseAccum} = 1$ since we only update a bit map. The second term is the storage requirement for the intermediate product, where the storage cost per fine-chunk storage is $s_{chunkFine} = s_{histoType} + s_{prefixSumType} + 2 * s_{cacheLine}$. The size of the histogram and prefix sum array data types are $s_{histoType}$ and $s_{prefixSumType}$ respectively. The $2 * s_{cacheLine}$ term accounts for the storage of active cache lines when non-sequentially writing to $colFine$ and $valFine$ during the reordering phase.

The value of $nChunksFine$ that minimizes Equation 3 is

$$nChunksFine_{opt} = \sqrt{\frac{m(C) * s_{denseAccum}}{s_{chunkFine}}}, \quad (4)$$

rounded to the nearest power of two. Plugging $nChunksFine_{opt}$ into Equation 3 we get

$$s_{fineLevel_{opt}} = 2\sqrt{m(C) * s_{denseAccum} * s_{chunkFine}} \quad (5)$$

for the total storage requirement of the fine-level algorithm. As $m(C)$ increases, $s_{fineLevel_{opt}}$ will eventually exceed s_{L2} and the coarse-level algorithm must be applied. In this case, we first determine $m(C)_{minL2}$, which is the minimum value of $m(C)$ such that $s_{fineLevel} < s_{L2}$. By solving $s_{fineLevel} = s_{L2}$ for $m(C)_{minL2}$ ($m(C)$ is replaced by the free parameter $m(C)_{minL2}$ in Equation 5), we get

$$m(C)_{minL2} = \frac{s_{L2}^2}{4 * s_{denseAccum} * s_{chunkFine}}, \quad (6)$$

floored to the nearest power of two. Plugging $m(C)_{minL2}$ into Equation 4 gives us the number of fine-level chunks, and

the number of coarse-level chunks is $m(C)/m(C)_{\min L2}$. In other words, we generate chunks of length $m(C)_{\min L2}$, and the fine-level algorithm is then applied to each coarse-level chunk.

Note that we only consider the minimizing for dense accumulation. This is because the sort-based accumulator does not require any additional storage since the arrays storing the intermediate product are directly sorted. The same analysis can be applied to other accumulators, e.g., hash maps.

IV. EXPERIMENTAL RESULTS

A. Test Configuration

In this section, we compare an OpenMP implementation of MAGNUS to several state-of-the-art SpGEMM algorithms. These baselines include Intel MKL [10], CSeg [2], and vectorized hash/heap-based algorithms [34], [35]. For MKL, we use the sparse BLAS inspector-executor API, i.e., the function `mkl_sparse_spm()`. For a fair comparison, we turned off matrix compression in CSeg. We report the *end-to-end* time for all SpGEMM algorithms, where the end-to-end time is the sum of the pre-processing, symbolic, and numeric phases. For example, the end-to-end time for CSeg is the sum of the time taken to construct the high-level summary matrix and perform the symbolic and numeric phases. In contrast, for MKL, we measure only the time of a single call to `mkl_sparse_spm()`, as that is the only operation exposed to us. We perform one warm-up run and then extract the time by taking the average of the next 10 runs. We found that the time did not vary significantly between many runs. Our test systems are shown in Table I, all of which use Intel x86 processors.

TABLE I

HARDWARE SPECIFICATIONS OF THE TEST SYSTEMS. ALL SYSTEMS ARE A SINGLE MULTI-SOCKET NODE WITH INTEL CPUS. ALL CPUS SUPPORT HYPERTHREADING.

Architecture	Skylake (SKL)	Sapphire Rapids (SPR)	Emerald Rapids (EMR)
Xeon Model	Gold 6140	Gold 6438M	Platinum 8592+
GHz	2.3	2.2	1.9
Sockets	4	2	2
Total cores and threads	72 and 144	64 and 128	128 and 256
L1 size per core	32 KB	48 KB	48 KB
L2 size per core	1 MB	2 MB	2 MB
L3 size per socket	24.75 MB	60 MB	320 MB
Memory	2 TB	4 TB	.5 TB

We consider three important matrix sets: matrices from the SuiteSparse collection [13], recursive model power law matrices (R-mats) [8], and uniform random matrices from the Erdős-Rényi (ER) model [16]. Table II shows the set of SuiteSparse matrices used in our experiments. These matrices are the largest 20 (in terms of the total number of non-zero values) in which both the input and output fit into memory for MAGNUS and at least one baseline on the SPR system. Table III show the R-mats with an average of 16 non-zeros per row, respectively, where the table is organized by increasing *scale*, e.g., rmat18 (a scale-18 R-mat) has 2^{18} rows. The standard Graph500 parameters were used to generate these R-mats ($a = .57$ and $b = c = .19$). The scale 23 matrix is the largest in which both the input and

TABLE II
PARAMETERS OF THE SUITESPARSE MATRIX COLLECTION.

Matrix	$n(A)$	$nnz(A)$	$nnz(A^2)$
kmer_U1a	67,716,231	138,778,562	222,262,359
kmer_P1a	139,353,211	297,829,984	531,367,449
kmer_A2a	170,728,175	360,585,172	622,660,207
kmer_V1r	214,005,017	465,410,904	824,450,881
vas_stokes_4M	4,382,246	131,577,616	826,486,449
rgg_n_2_24_s0	16,777,216	265,114,400	828,639,073
nlpkkt160	8,345,600	229,518,112	1,241,294,184
Queen_4147	4,147,110	329,499,284	1,501,950,816
HV15R	2,017,169	283,073,458	1,768,066,720
indochina-2004	7,414,866	194,109,311	1,952,630,542
stokes	11,449,533	349,321,980	2,115,146,825
nlpkkt200	16,240,000	448,225,632	2,425,937,704
uk-2002	18,520,486	298,113,762	3,194,986,138
nlpkkt240	27,993,600	774,472,352	4,193,781,224
arabic-2005	22,744,080	639,999,458	8,323,612,632
uk-2005	39,459,925	936,364,282	8,972,400,198
webbase-2001	118,142,155	1,019,903,190	13,466,717,166
it-2004	41,291,594	1,150,725,436	14,045,664,641
mycielskian18	196,607	300,933,832	38,353,378,617
com-Orkut	3,072,441	234,370,166	49,836,711,933

TABLE III

PARAMETERS OF THE R-MAT16 MATRIX SET (R-MAT WITH AN AVERAGE OF 16 NON-ZEROS PER ROW). THE OPTIMAL NUMBER OF CHUNKS USED IN MAGNUS IS SHOWN IN THE LAST COLUMN.

Matrix	$n(A)$	$nnz(A)$	$nnz(A^2)$	
rmat18	262,144	4,194,304	1,347,858,618	
rmat19	524,288	8,388,608	3,708,083,907	
rmat20	1,048,576	16,777,216	9,940,402,266	
rmat21	2,097,152	33,554,432	25,958,392,028	
rmat22	4,194,304	67,108,864	68,732,382,095	
rmat23	8,388,608	134,217,728	186,673,674,064	

output fit into memory for MAGNUS and at least one baseline on the SPR system. For the SuiteSparse and R-mat sets, we consider the operation A^2 , which is common practice for testing SpGEMM algorithms, where A is a square matrix. Lastly, the configuration for the ER matrix set will be discussed later in this section. Before presenting our SpGEMM results, we first show microbenchmark results for the important building blocks of MAGNUS.

B. Microbenchmarks

The purpose of this section is to establish the motivation for MAGNUS by testing its various building blocks. We first show that increasing the size and length of the intermediate product degrades the performance of conventional accumulators. We then benchmark the building blocks of MAGNUS to show how the introduction of locality generation can improve the performance of the accumulator. For these experiments, four-byte types were used (`uint32_t` and `float`) on one core of the SPR system.

1) Accumulators

We first consider the two accumulators used by MAGNUS: AVX-512 vectorized bitonic sorting [7] and dense accumulation. The goal is to identify their strengths and weaknesses by

performing accumulation on a random input stream. The input stream consists of two vectors, one of unsigned integers (*idx* stream) and the other of floating point numbers (*val* stream), which represent the column indices and values, respectively, in the intermediate product of a C row. There are two important parameters to consider: the number of elements in each vector (we will refer to this as the stream *size*), and the maximum value of the elements in the *idx* array (we will refer to this as *max index*). In general, SpGEMM accumulators are sensitive to these two parameters. We do not consider merging, just the accumulation step. This means that for sorting, we only consider the actual sort time and not the second step in which we walk through the sorted sequence and eliminate duplicates. For dense accumulation, we only update the dense value vector and companion bitmap.

Figure 4 shows results for the benchmark, where both subfigures measure the rate (in millions per second) at which the elements in the stream are accumulated. The top subfigure shows the effect of increasing the stream size from 0 to 512 with a fixed max index of $2^{17} - 1$, the maximum index for which the dense accumulator data structures fit into the L2 cache. There are two important sort sizes to note: 32 and 256. At 32, the sorting achieves peak performance at just under 700 million elements per second. This suggests that we should try to get the sorting sizes as close to 32 as possible. In MAGNUS, we do exactly this: we combine consecutive chunks until the difference between the sort size and 32 is minimized. Dense accumulation overtakes sorting at a stream size of 256 and is $\approx 1.5\times$ faster for a sort size of 512. The 256 threshold comes from the sorting algorithm, which partitions the array into 256 parts (for more information, see [7]). This is exactly the threshold we use in our code when choosing an accumulator within a chunk. The bottom subfigure shows the effect of increasing the maximum index beyond 2^{17} such that the dense accumulation data structures do not fit into cache. The stream size is fixed, which is why the sorting rate does not change. The dashed line shows the point at which the performance of dense accumulation drops off. Note that with larger stream sizes the flat line for sorting performance will continually drop lower, as demonstrated in the first subfigure.

There are two important conclusions: if the maximum index and stream size are both large, both accumulators will perform suboptimally. Therefore, it is advantageous to reorganize the intermediate product of C such that both these quantities are reduced. This motivates the use of the locality-generation algorithms in MAGNUS, which address the two above problems by reordering the intermediate product into discrete chunks of smaller length than the input. Since each chunk can be processed independently, sorting will perform well if enough chunks are used. If the column indices in the intermediate product are not uniform, resulting in chunks with many elements, the dense accumulator can be applied. If enough chunks are used, the maximum index of each chunk will be small enough such that the dense accumulator data structures fit into cache.

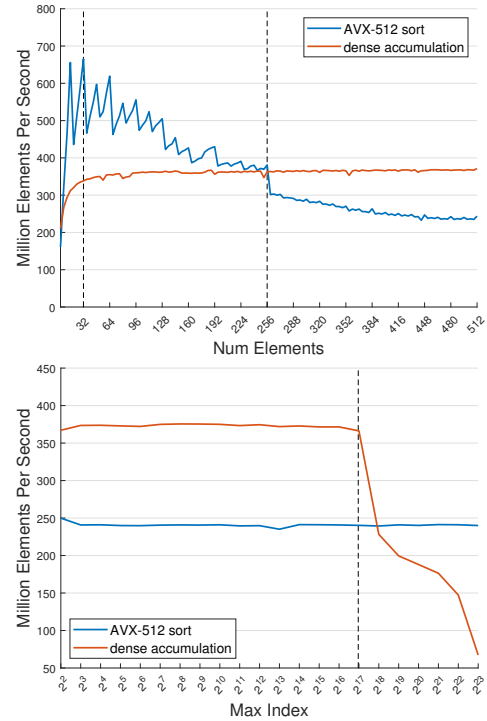


Fig. 4. Comparison of accumulators used in MAGNUS: AVX-512 vectorized sorting and dense accumulation on a single core of the SPR system. The rate (millions of elements per second) as a function of the number of elements is shown in the top subfigure. The dashed lines indicate where the sorting achieves peak performance (32 elements) and where the performance of dense accumulation overtakes that of sorting (256 elements). In the bottom subfigure shows the rate versus the max index. The dashed line denotes the maximum size of the accumulator such that it fits into cache.

2) Building Blocks of MAGNUS

In this experiment, MAGNUS is deconstructed into its building blocks and tested using random input streams, as in the previous microbenchmarks. The building blocks are histogramming, prefix summing, reordering, and accumulation. Figure 5 shows time versus number of chunks for a stream size of 2^{29} . The number of chunks varies from 1 to 2^{20} . For dense accumulation, the maximum index varies from 2^{29} to $2^{29}/2^{20} = 512$ to emulate the per-chunk dense accumulation in MAGNUS. Unlike in Section IV-B1, the time for writing the output is included in the accumulation such that the total time (sum of the building block times) includes writing. The horizontal dashed line shows the performance of sequentially loading and storing the stream, i.e., a standard streaming benchmark, which serves as our peak performance baseline, where the sum of the building block times cannot exceed this baseline. The vertical dashed line shows the optimal number of chunks for the fine-level algorithm in MAGNUS, which is computed using the maximum index as $m(C)$.

The dominant cost for histogramming comes from just reading the input integer stream and updating the cached histogram, which is inexpensive compared to reordering. The reordering time increases significantly past 2^{12} , where the storage requirement (active cache lines, histogram array, and prefix sum array) exceeds the L2 cache size. Beyond 2^{18} chunks, the L3 cache size is exceeded, resulting in another

drop-off in performance. For dense accumulation, performance improves as the number of chunks increases since the maximum index decreases, as previously shown in Section IV-B1. The total time is the sum of the building block times and has a minimum at the optimal number of fine-level chunks. At this number of chunks, the total time is ≈ 2 the load-store time, which is our peak performance baseline. Although lower-level optimizations have the potential to further close this gap (e.g., vectorized histogramming), the goal of MAGNUS is to maintain a reasonable multiple of the peak performance as the matrix size scales up. We will show in Section IV-C that MAGNUS can maintain a small multiple of the peak performance for massive random matrices, while other SpGEMM baselines cannot.

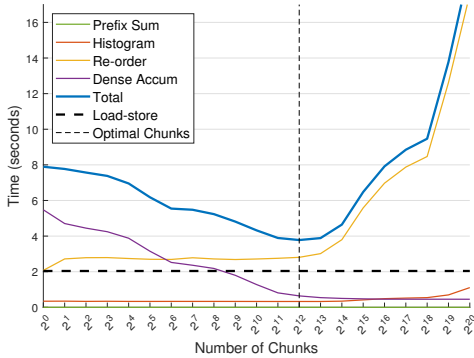


Fig. 5. Wall-clock time versus number of chunks for a set of microbenchmarks that test the performance of the building blocks of MAGNUS. The input is a stream of uniform random unsigned integers in the range $[0, 2^{29} - 1]$ paired with a stream of random floating point values. The sum of the building block times is also shown, and the performance of sequentially loading and storing the input stream serves as a peak-performance baseline. The vertical dashed line denotes the optimal number of fine-level chunks based on the stream length.

C. SpGEMM

For our SpGEMM experiments, we used all available threads (including hyperthreads) on all our systems. For the first set of SpGEMM results, we consider the SuiteSparse matrix collection. Figure 6 shows the time in logarithmic scale for each matrix and each system. In some cases, out-of-memory errors and segmentation faults caused some of the baselines to fail, denoted by the missing bars. The reason com-Orkut is not shown in the EMR results is because C does not fit in memory, resulting in MAGNUS and all baselines failing. MAGNUS is often faster than all baselines and is often orders of magnitude faster than MKL, a state-of-the-art library. CSeg is slightly faster than MAGNUS (up to $1.26\times$) for three cases: Queen_4147 and HV15R on all systems, and rgg_n_2_24_s0 on just SPR. In MAGNUS, all rows are placed into the dense accumulation category for these matrices, i.e., these matrices do not require locality generation to be efficiently multiplied. Similarly, the kmer matrices also do not require locality generation, where Hash and Heap are slightly faster for kmer_P1a on SKL. These matrices are not banded but are highly sparse, leading to an intermediate product per row that

is less than our dense accumulation threshold. Therefore, sort- or hash map-based accumulators are most effective, as shown by MAGNUS and Hash/Heap having the fastest times (most rows in MAGNUS are placed into the sort category). In all other cases, rows are categorized with a mix of sorting, dense accumulation, and fine-level locality in MAGNUS, where a significant number of rows are categorized for the fine-level algorithm (the number of columns of C is too small to use the coarse-level algorithm). For these matrices, MAGNUS is up to 17.5, 306.6, 174, and 2.25 times faster than CSeg, MKL, Hash, and Heap, respectively.

For the remaining experiments, we only consider the SPR system, which has the largest memory capacity. Comparing across multiple systems does not provide additional insight into the behavior of MAGNUS since we cannot scale up the L2 cache size like we can with the matrix size. Figure 7 shows the wall clock time and speedup versus the number of rows for the RMat16 matrix set. Since we are using the standard Graph500 parameters, a small average number of non-zeros per row (16 in this case) produces high fill-in in C (as shown in Table III) since many of the non-zeros in the input matrices are clustered in the top left corner of A and B . Unlike banded and other highly sparse structures that produce moderate fill-in, this mix of a random distribution with clustering in the R-mats is problematic for conventional accumulators since a high data volume across a wide range of column indices results in data structures that do not fit into cache. This is demonstrated in Figure 7, which shows the poor scaling of MKL as the number of rows increases (MKL failed for the two largest cases). Compared to MAGNUS, the performance of MKL degrades as the number of rows increases, where MAGNUS is more than 6 times faster than MKL for the largest matrix. Heap failed in all cases, and Hash failed in all but the smallest case. The scaling of CSeg and MAGNUS demonstrates the importance of locality generation as we scale up the size of the matrix. Although MAGNUS is $\approx 1.8 - 2$ times faster than CSeg, they both scale at a similar rate, unlike MKL.

Lastly, we explore experiments on uniform random matrices (i.e., matrices from the Erdős-Rényi (ER) model). Unlike the R-mats, a small number of non-zeros per row does not produce a massive fill-in, and the fill-in is evenly distributed unlike the clustering of the R-mats. As we scale up the number of columns of C and non-zeros per row, the uniform distribution of the column indices results in frequent reading and writing to the entire accumulation data structure. For conventional accumulators, this becomes cache inefficient if no locality generation strategy is used. Since the performance of accumulators is sensitive to the number of columns of C and not the number of rows, we consider the non-square case where C has 2048 rows and a variable number of columns. This allows us to scale to massive matrices without exceeding the memory limit of our system. Additionally, only the rows of B that depend on the non-zeros in A are generated, which saves additional memory.

We first consider a fixed number of columns of 2^{24} and a variable average number of non-zeros per row, as shown in

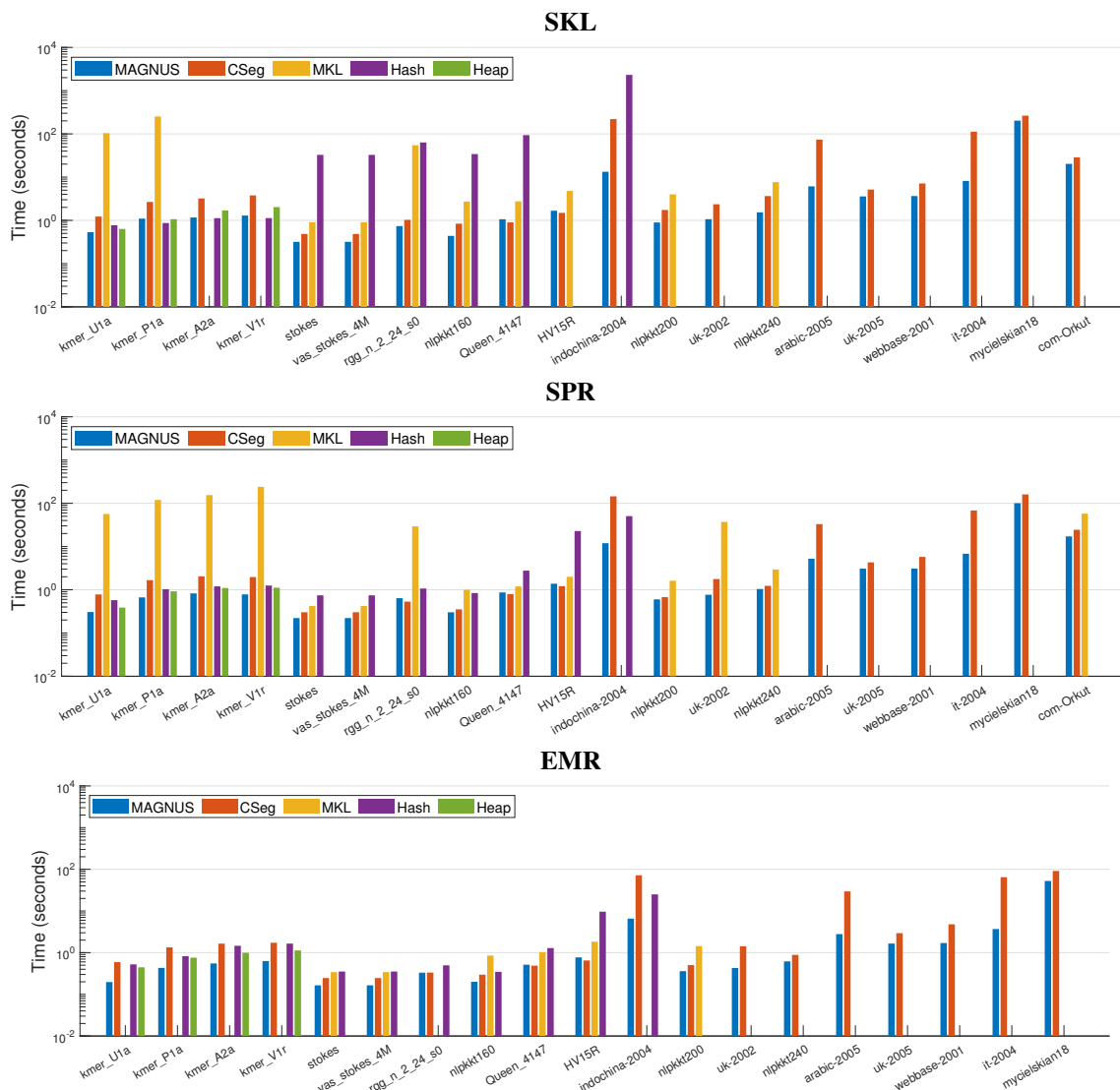


Fig. 6. Wall-clock time in log scale for the SuiteSparse matrix collection. All available threads were used for each system. The figure titles denote the different test systems (see Table I).

the top subfigure of Figure 8, where the black line is the ideal performance bound. This bound was calculated by dividing the read and write data volumes by the system bandwidth, which was measured using a streaming benchmark. This bound does not account for various costs, such as floating-point operations, NUMA effects, or synchronization overheads, which can be significant in any SpGEMM algorithm. Except for the two smallest cases, MAGNUS is faster than all the baselines (Heap failed in all cases). The two smallest cases show the benefit of hash-based accumulators which are efficient for highly-sparse inputs. However, Hash scales poorly with the number of non-zeros. CSeg and MAGNUS are the fastest for the largest inputs and generally scale better than MKL and Hash, showing that increasing the number of non-zeros per row requires a locality-generation strategy.

The bottom subfigure in Figure 8 shows results for increasing the number of columns with a fixed average number of non-

zeros per row of 4096. MKL, Hash, and Heap failed in all cases. The slight increase in the ideal bound at 2^{32} is due to a change from four- to eight-byte data types for the column indices. The results show that CSeg’s method of locality generation, where an auxiliary segmented matrix is explicitly constructed, does not scale to large numbers of columns. In the worst case, MAGNUS is more than four times faster than CSeg, which fails for numbers of columns above 2^{31} . MAGNUS is able to sustain a multiple of ≈ 2 the ideal bound before the coarse-level algorithm is applied, and ≈ 3 after (the increase in the multiple is due to the increase in data volume incurred by the outer product-based coarse-level algorithm), while CSeg diverges from the bound. The vertical dashed line shows the point at which MAGNUS starts to place rows in the coarse-level category. The dashed blue line shows MAGNUS with the coarse-level algorithm turned off. This shows the necessity of multiple levels of locality, especially for massive matrices

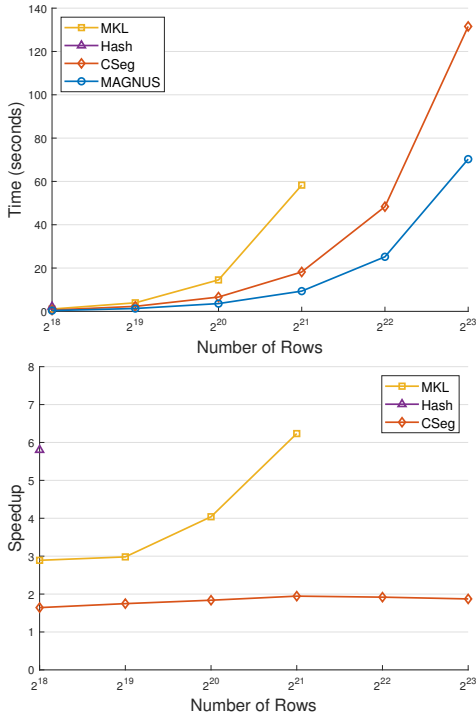


Fig. 7. Wall-clock time and speedup versus number of rows for the RMat16 matrix set on the SPR system.

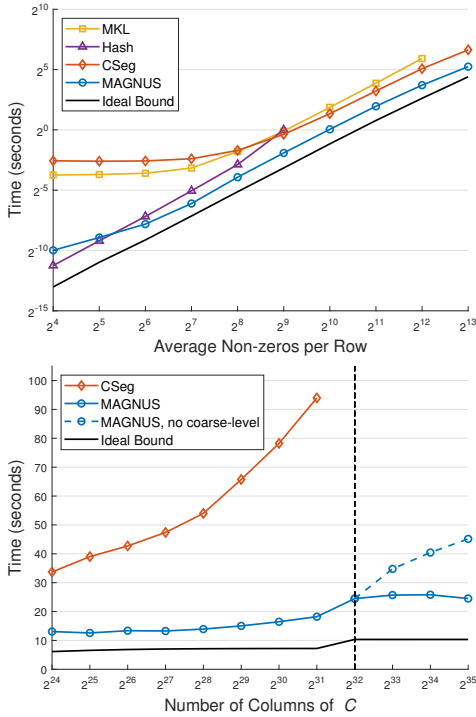


Fig. 8. Results for matrices from the Erdős-Rényi (ER) model (i.e., uniform random matrices) on the SPR system. The top subfigure shows time versus average number of non-zeros per row for a fixed number of columns of C of 2^{24} . The bottom subfigure shows time vs number of columns of C for a fixed average number of non-zeros per row of 4096. We consider the non-square case where the number of rows of C is 2048 such that we can scale up to 2^{35} columns of C and stay within the memory limit of our system. The vertical dashed line denotes the point at which MAGNUS starts using the coarse-level algorithm.

where the fine-level algorithm data structures do not fit into cache.

V. CONCLUSION

On modern multi-core architectures, current SpGEMM algorithms often scale poorly to massive matrices due to inefficient use of the cache hierarchy. We present MAGNUS, a novel algorithm for locality generation, where the intermediate product is reordered into cache-friendly chunks using a hierarchical two-level approach. MAGNUS consists of two algorithms that create multiple levels of locality: the fine- and coarse-level algorithms. The coarse-level algorithm generates a set of cache-friendly chunks, and the fine-level algorithm further subdivides the coarse-level chunks to maximize the performance of the accumulators. Experimental results are presented that compare MAGNUS with several baselines for three different matrix sets on three different Intel x86 architectures. MAGNUS is faster than all the baselines in most cases and is sometimes orders of magnitude faster than Intel MKL. More importantly, MAGNUS scales to massive uniform random matrices, which is the most challenging test set that we consider. This challenging case demonstrates the need for the coarse-level algorithm, which allows MAGNUS to scale to the largest matrices. Specifically, the coarse-level algorithm allows MAGNUS to stay within an ideal performance bound, regardless of the matrix properties, while the baselines diverge from the bound as the matrix size increases.

REFERENCES

- [1] Rasmus Amossen, Andrea Campagna, and Rasmus Pagh. Better size estimation for sparse matrix products. *Algorithmica*, 69:741–757, March 2013.
- [2] Xiaojing An and Ümit V. Çatalyürek. Column-segmented sparse matrix-matrix multiplication on multicore cpus. In *2021 IEEE 28th International Conference on High Performance Computing, Data, and Analytics (HiPC)*, pages 202–211, December 2021.
- [3] Pham Nguyen Quang Anh, Rui Fan, and Yonggang Wen. Balanced hashing and efficient GPU sparse general matrix-matrix multiplication. In *Proceedings of the 2016 International Conference on Supercomputing*, New York, NY, USA, 2016. Association for Computing Machinery.
- [4] Ariful Azad, Grey Ballard, Aydin Buluç, James Demmel, Laura Grigori, Oded Schwartz, Sivan Toledo, and Samuel Williams. Exploiting multiple levels of parallelism in sparse matrix-matrix multiplication. *SIAM Journal on Scientific Computing*, 38(6):C624–C651, 2016.
- [5] Ariful Azad, Aydin Buluç, and John Gilbert. Parallel triangle counting and enumeration using matrix algebra. In *2015 IEEE International Parallel and Distributed Processing Symposium Workshop*, pages 804–811, 2015.
- [6] Ariful Azad, Georgios A Pavlopoulos, Christos A Ouzounis, Nikos C Kyrpides, and Aydin Buluç. HipMCL: a high-performance parallel implementation of the Markov clustering algorithm for large-scale networks. *Nucleic Acids Research*, 46(6):e33–e33, January 2018.
- [7] Berenger Bramas. A novel hybrid quicksort algorithm vectorized using AVX-512 on Intel Skylake. *International Journal of Advanced Computer Science and Applications*, 8(10), 2017.
- [8] Deepayan Chakrabarti, Yiping Zhan, and Christos Faloutsos. *R-MAT: A Recursive Model for Graph Mining*, pages 442–446. SIAM, 2004.
- [9] Helin Cheng, Wenxuan Li, Yuechen Lu, and Weifeng Liu. HASpGEMM: Heterogeneity-aware sparse general matrix-matrix multiplication on modern asymmetric multicore processors. In *Proceedings of the 52nd International Conference on Parallel Processing, ICPP '23*, page 807–817, New York, NY, USA, 2023. Association for Computing Machinery.
- [10] Intel Corporation. Developer reference for Intel oneAPI math kernel library (MKL) for C, 2023.
- [11] NVIDIA Corporation. cusparse library, 2023.

- [12] Steven Dalton, Luke Olson, and Nathan Bell. Optimizing sparse matrix-matrix multiplication for the GPU. *ACM Transactions on Mathematical Software*, 41(4), October 2015.
- [13] Timothy A. Davis and Yifan Hu. The university of florida sparse matrix collection. *ACM Transactions on Mathematical Software*, 38(1), December 2011.
- [14] Mehmet Deveci, Christian Trott, and Siva Rajamanickam. Multi-threaded sparse matrix-matrix multiplication for many-core and GPU architectures. *Parallel Computing*, 78, January 2018.
- [15] Zhaoyang Du, Yijin Guan, Tianchan Guan, Dimin Niu, Linyong Huang, Hongzhong Zheng, and Yuan Xie. OpSparse: A highly optimized framework for sparse general matrix multiplication on GPUs. *IEEE Access*, 10:85960–85974, 2022.
- [16] P. Erdős and A. Rényi. On random graphs I. *Publicationes Mathematicae Debrecen*, 6:290, 1959.
- [17] R.D. Falgout. An introduction to algebraic multigrid. *Computing in Science & Engineering*, 8(6):24–33, 2006.
- [18] Xu Feng, Yuyang Xie, Mingye Song, Wenjian Yu, and Jie Tang. Fast randomized PCA for sparse data. In *Asian conference on machine learning*, pages 710–725. PMLR, 2018.
- [19] Jianhua Gao, Weixing Ji, Fangli Chang, Shiyu Han, Bingxin Wei, Zeming Liu, and Yizhuo Wang. A systematic survey of general sparse matrix-matrix multiplication. *ACM Computing Surveys*, 55(12), March 2023.
- [20] John Gilbert, Cleve Moler, and Robert Schreiber. Sparse matrices in MATLAB: Design and implementation. *SIAM Journal on Matrix Analysis and Applications*, 13, May 1997.
- [21] John R. Gilbert, Steve Reinhardt, and Viral B. Shah. High-performance graph algorithms from parallel sparse matrices. In *Applied Parallel Computing: State of the Art in Scientific Computing*, pages 260–269, Berlin, Heidelberg, 2007. Springer Berlin Heidelberg.
- [22] Vitaliy Gleyzer, Andrew J. Soszynski, and Edward K. Kao. Leveraging linear algebra to count and enumerate simple subgraphs. In *2020 IEEE High Performance Extreme Computing Conference (HPEC)*, pages 1–8, 2020.
- [23] Zhixiang Gu, Jose Moreira, David Edelsohn, and Ariful Azad. Bandwidth optimized parallel algorithms for sparse matrix-matrix multiplication using propagation blocking. In *Proceedings of the 32nd ACM Symposium on Parallelism in Algorithms and Architectures*, SPAA '20, page 293–303, New York, NY, USA, 2020. Association for Computing Machinery.
- [24] Giulia Guidi, Marquita Ellis, Daniel Rokhsar, Katherine Yelick, and Aydın Buluç. *BELLA: Berkeley Efficient Long-Read to Long-Read Aligner and Overlapper*, pages 123–134. 2021.
- [25] Giulia Guidi, Oguz Selvitopi, Marquita Ellis, Leonid Oliker, Katherine A. Yelick, and Aydın Buluç. Parallel string graph construction and transitive reduction for de novo genome assembly. In *2021 IEEE International Parallel and Distributed Processing Symposium (IPDPS)*, pages 517–526, Los Alamitos, CA, USA, May 2021. IEEE Computer Society.
- [26] Fred G. Gustavson. Two fast algorithms for sparse matrices: Multiplication and permuted transposition. *ACM Transactions on Mathematical Software*, 4(3):250–269, September 1978.
- [27] Haim Kaplan, Micha Sharir, and Elad Verbin. Colored intersection searching via sparse rectangular matrix multiplication. In *Proceedings of the Twenty-Second Annual Symposium on Computational Geometry*, SCG '06, page 52–60, New York, NY, USA, 2006. Association for Computing Machinery.
- [28] Valentin Le Fèvre and Marc Casas. Efficient execution of SpGEMM on long vector architectures. In *Proceedings of the 32nd International Symposium on High-Performance Parallel and Distributed Computing*, HPDC '23, page 101–113, New York, NY, USA, 2023. Association for Computing Machinery.
- [29] Jiayu Li, Fugang Wang, Takuya Araki, and Judy Qiu. Generalized sparse matrix-matrix multiplication for vector engines and graph applications. In *2019 IEEE/ACM Workshop on Memory Centric High Performance Computing (MCHPC)*, pages 33–42, 2019.
- [30] Ruipeng Li, Björn Sjögreen, and Ulrike Meier Yang. A new class of amg interpolation methods based on matrix-matrix multiplications. *SIAM Journal on Scientific Computing*, 43(5):S540–S564, 2021.
- [31] Junhong Liu, Xin He, Weifeng Liu, and Guangming Tan. Register-aware optimizations for parallel sparse matrix-matrix multiplication. *Int. J. Parallel Program.*, 47(3):403–417, June 2019.
- [32] Weifeng Liu and Brian Vinter. An efficient GPU general sparse matrix-matrix multiplication for irregular data. In *2014 IEEE 28th International Parallel and Distributed Processing Symposium*, pages 370–381, 2014.
- [33] Weifeng Liu and Brian Vinter. A framework for general sparse matrix-matrix multiplication on GPUs and heterogeneous processors. *Journal of Parallel and Distributed Computing*, 85:47–61, 2015. IPDPS 2014 Selected Papers on Numerical and Combinatorial Algorithms.
- [34] Yusuke Nagasaka, Satoshi Matsuoka, Ariful Azad, and Aydın Buluç. High-performance sparse matrix-matrix products on Intel KNL and multicore architectures. In *Workshop Proceedings of the 47th International Conference on Parallel Processing, ICPP Workshops '18*, New York, NY, USA, 2018. Association for Computing Machinery.
- [35] Yusuke Nagasaka, Satoshi Matsuoka, Ariful Azad, and Aydın Buluç. Performance optimization, modeling and analysis of sparse matrix-matrix products on multi-core and many-core processors. *Parallel Computing*, 90:102545, 2019.
- [36] Yusuke Nagasaka, Akira Nukada, and Satoshi Matsuoka. High-performance and memory-saving sparse general matrix-matrix multiplication for NVIDIA Pascal GPU. In *2017 46th International Conference on Parallel Processing (ICPP)*, pages 101–110, 2017.
- [37] Mathias Parger, Martin Winter, Daniel Mlakar, and Markus Steinberger. spECK: accelerating GPU sparse matrix-matrix multiplication through lightweight analysis. In *Proceedings of the 25th ACM SIGPLAN Symposium on Principles and Practice of Parallel Programming*, PPoPP '20, page 362–375, New York, NY, USA, 2020. Association for Computing Machinery.
- [38] Md. Mostofa Ali Patwary, Nadathur Rajagopalan Satish, Narayanan Sundaram, Jongsoo Park, Michael J. Anderson, Satya Gautam Vadlamudi, Dipankar Das, Sergey G. Pudov, Vadim O. Pirogov, and Pradeep Dubey. Parallel efficient sparse matrix-matrix multiplication on multicore platforms. In *High Performance Computing*, pages 48–57, Cham, 2015. Springer International Publishing.
- [39] Eric Qin, Ananda Samajdar, Hyoukjun Kwon, Vineet Nadella, Dipankar Srinivasan, Sudarshan an Das, Bharat Kaul, and Tushar Krishna. SIGMA: A sparse and irregular GEMM accelerator with flexible interconnects for DNN training. In *2020 IEEE International Symposium on High Performance Computer Architecture (HPCA)*, pages 58–70, 2020.
- [40] Oguz Selvitopi, Md Taufique Hussain, Ariful Azad, and Aydın Buluç. Optimizing high performance markov clustering for pre-exascale architectures. In *2020 IEEE International Parallel and Distributed Processing Symposium (IPDPS)*, pages 116–126, 2020.
- [41] Hikaru Takayashiki, Hotaka Yagi, Hiroki Nishimoto, and Naoki Yoshifuji. A new sparse general matrix-matrix multiplication method for long vector architecture by hierarchical row merging. In *Proceedings of the SC '23 Workshops of The International Conference on High Performance Computing, Network, Storage, and Analysis*, SC-W '23, page 756–759, New York, NY, USA, 2023. Association for Computing Machinery.
- [42] Martin Winter, Daniel Mlakar, Rhaleb Zayer, Hans-Peter Seidel, and Markus Steinberger. Adaptive sparse matrix-matrix multiplication on the GPU. In *Proceedings of the 24th Symposium on Principles and Practice of Parallel Programming*, PPoPP '19, page 68–81, New York, NY, USA, 2019. Association for Computing Machinery.
- [43] Michael M. Wolf, Jonathan W. Berry, and Dylan T. Stark. A task-based linear algebra building blocks approach for scalable graph analytics. In *2015 IEEE High Performance Extreme Computing Conference (HPEC)*, pages 1–6, 2015.
- [44] Kathy Yelick, Aydın Buluç, Muaaz Awan, Ariful Azad, Bowei Brock, Rob Egan, Saliya Ekanayake, Marquita Ellis, Evangelos Georganas, Giulia Guidi, Steven Hofmeyr, Oguz Selvitopi, Cristina Teodoropol, and Leonid Oliker. The parallelism motifs of genomic data analysis. *Philosophical Transactions of the Royal Society A: Mathematical, Physical and Engineering Sciences*, 378(2166):20190394, 2020.
- [45] Chao Zhang, Maximilian Bremer, Cy Chan, John Shalf, and Xiaochen Guo. ASA: Accelerating sparse accumulation in column-wise SpGEMM. *ACM Transactions on Architecture and Code Optimization*, 19(4), September 2022.
- [46] Guowei Zhang, Nithya Attaluri, Joel S. Emer, and Daniel Sanchez. GAMMA: leveraging Gustavson's algorithm to accelerate sparse matrix multiplication. In *Proceedings of the 26th ACM International Conference on Architectural Support for Programming Languages and Operating Systems*, ASPLOS '21, page 687–701, New York, NY, USA, 2021. Association for Computing Machinery.